

pathological masses in that age group<sup>(4,5)</sup>. It is relatively rare in the pediatric population. The symptoms are nonspecific and, due to the rarity of this condition in pediatric patients, etiologies such as appendicitis, diverticulitis, and renal colic are more likely explanations for the clinical symptoms than is ovarian torsion. Ultrasound is the first-line imaging modality in any case of acute abdomen.

One study showed that ultrasound has a positive predictive value of 87.5% and a specificity of 93.3% for the diagnosis of ovarian masses, as well as having other advantages such as low cost, easy accessibility, and no radiation<sup>(6)</sup>. On gray-scale imaging, the affected ovary appears enlarged, increasing to up to 28 times its original size<sup>(7)</sup>. The diagnostic criteria for enlarged ovaries include an ovarian diameter of > 4 cm or volume > 20 mL in women of reproductive age and > 10 mL in postmenopausal women<sup>(8,9)</sup>. Cystic or solid masses can also be identified on ultrasound. Cysts can show wall thickening. Free fluid can be seen in the pelvic cavity. The twisted vascular pedicle is typically seen as an echogenic round or beaked mass with multiple concentric, hypoechoic, target-like stripes. It can also appear as an ellipsoid or tubular mass with internal heterogeneous echoes, depending on the plane of orientation. Although color Doppler typically shows the absence of arterial flow, the presence of arterial flow does not rule out the possibility of torsion, because the arteries are affected at a later stage and there can be arterial supply from the uterine arteries as well. The twisted vascular pedicle can give rise to the whirlpool sign on color Doppler.


REFERENCES

1. Pedrosa I, Zeikus EA, Levine D. MR imaging of acute right lower quadrant pain in pregnant and nonpregnant patients. *Radiographics*. 2007;27:721–43; discussion 743–53.
2. Hibbard LT. Adnexal torsion. *Am J Obstet Gynecol*. 1985;152:456–61.
3. Albayram F, Hamper UM. Ovarian and adnexal torsion: spectrum of sonographic findings with pathologic correlation. *J Ultrasound Med*. 2001;20:1083–9.
4. Chiou SY, Lev-Toaff AS, Masuda E, et al. New clinical and imaging observations by sonography, computed tomography, and magnetic resonance imaging. *J Ultrasound Med*. 2007;26:1289–301.
5. Gorkemli H, Camus M, Clasen K. Adnexal torsion after gonadotrophin ovulation induction for IVF or ICSI and its conservative treatment. *Arch Gynecol Obstet*. 2002;267:4–6.
6. Graif M, Itzhak Y. Sonographic evaluation of ovarian torsion in childhood and adolescence. *AJR Am J Roentgenol*. 1988;150:647–9.
7. Graif M, Shalev J, Strauss S, et al. Torsion of the ovary: sonographic features. *AJR Am J Roentgenol*. 1984;143:1331–4.
8. Chang HC, Bhatt S, Dogra VS. Pearls and pitfalls in diagnosis of ovarian torsion. *Radiographics*. 2008;28:1355–68.
9. Pavlik EJ, DePriest PD, Gallion HH, et al. Ovarian volume related to age. *Gynecol Oncol*. 2000;77:410–2.

Chiyarath Gopalan Muralidharan<sup>1</sup>, Shyam Krishna<sup>1</sup>, Tony Jose<sup>2</sup>

1. Command Hospital (SC) Pune, Maharashtra, India. 2. Armed Forces Medical College, Pune, Maharashtra, India. Mailing address: Chiyarath Gopalan Muralidharan, MD, Department of Radiodiagnosis, Command Hospital (SC) Pune, Maharashtra-411040, India. E-mail: murali.cg@rediffmail.com.

<http://dx.doi.org/10.1590/0100-3984.2016.0227>

 This is an open-access article distributed under the terms of the Creative Commons Attribution License.

**Asymptomatic apical aneurysm of the left ventricle with intracavitary thrombus: a diagnosis missed by echocardiography**

Dear Editor,

We report the case of a 63-year-old male, with a history of acute myocardial infarction (AMI) and angioplasty 10 years prior, who was asymptomatic at presentation. He stated that he had not undergone routine clinical follow-up and was therefore submitted to echocardiography for functional evaluation. Moderate dilation and dysfunction of the left ventricle (LV) were detected, although with limitation in the evaluation of the apex, without information on the presence of an aneurysm or thrombus. Coronary computed tomography angiography (CCTA) was performed in order to identify in-stent restenosis, and the images showed apparent subocclusion distal to the stent in the anterior descending artery (Figure 1A) and a large aneurysm with parietal thinning in the anterior/anteroapical medial segments, septal/

anterior apical segments, and apex of the LV. It was not possible to detect significant systolic ballooning, because there was a large thrombus lining the intracavitary portion and that was confused with normal wall thickness of the LV. The thrombus had an organized appearance, albeit without signs of calcification, and was markedly hypodense, with a fixed aspect and no contrast enhancement, which had likely made it difficult to identify in the initial (echocardiographic) assessment (Figures 1B and 1C).

Ventricular aneurysm is a serious complication of transmural myocardial infarction (occurring in 5–38% of cases), being the most common mechanical complication, typically evolving to physical limitations and having a negative impact on quality of life<sup>(1–4)</sup>. It is defined as myocardial ventricular wall thinning and dilation, with distinct margins, leading to akinesia or dyskinesia of one or more myocardial segments during ventricular contraction<sup>(1,2–5)</sup>. It typically affects the anteroapical region of the LV, because the blood supply of the anterior wall is highly

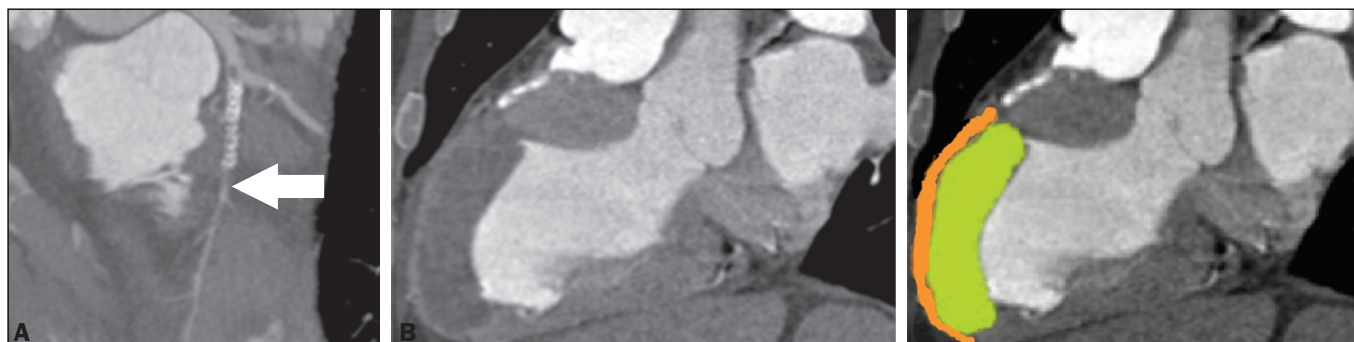


**Figure 1.** A: CCTA with a reconstruction curve showing probable subocclusion downstream of the stent (arrow). B,C: Cardiac computed tomography of the heart in the longitudinal axial plane, in a pseudo-two-chamber view, showing the region of the LV aneurysm with marked thinning of the medioapical anterior wall (2 mm thick – orange) and normal thickness in the anterior basal segment. Note the large thrombus simulating normal wall thickness of the LV (green).

dependent on the anterior descending artery<sup>(2,3)</sup>. Ventricular aneurysm develops within two to ten days after AMI, becoming apparent in the first year after the infarction, with an incidence of 30–35% in patients who have experienced AMI<sup>(4–6)</sup>. As a secondary finding, intracavitary thrombus affects approximately 40–60% of patients<sup>(4)</sup> and results from the inflammatory process in the endocardial region affected by the AMI, being associated with the hypokinesia and hypercoagulability existing in the infarction, increasing the risk of a thromboembolic event after the third month in patients with ventricular aneurysm. There is a broad range of symptoms in LV aneurysms, ranging from none to dyspnea, heart failure, or angina, as well as severe manifestations such as acute pulmonary edema, thromboembolism, and ventricular rupture<sup>(5–7)</sup>. In the treatment of severe refractory cases, surgical procedures, such as plication, excision/suture, imbrication, and patch interposition, are indicated<sup>(8)</sup>. In the case presented here, despite the extensive area of left ventricular dyskinesia with aneurysm formation and adherent intracavitary thrombus, the patient remained asymptomatic, an uncommon presentation in large aneurysms, which was diagnosed only through CCTA, a noninvasive method that not only allows the diagnosis to be made but also provides accurate measurements and can be used in the postoperative follow-up<sup>(1,4–6,9–11)</sup>. Routine screening tests, such as echocardiography, often fail to assess the apex of the LV, even with a good access window<sup>(1,2,7)</sup>. In addition to allowing the diagnosis to be made, the CCTA findings promoted patient adherence to the treatment.

## REFERENCES

- Assunção FB, Oliveira DC, Souza VF, et al. Cardiac magnetic resonance imaging and computed tomography in ischemic cardiomyopathy: an update. *Radiol Bras.* 2016;49:26–34.
- Cardoso MB, Azevedo CHNF, Teixeira CO, et al. Aneurisma do ventrículo

- esquerdo pós-infarto do miocárdio: correlação da semiotécnica complementar com os achados anatomopatológicos: relato de quatro casos com necropsia. *Rev Ciênc Méd, Campinas.* 2001;10: 31–5.
- Debray M, Pautas E, Dulou L, et al. Aneurysm of the left ventricle: a two-decade silent history. *J Am Geriatr Soc.* 2001;49:337–8.
- Strecker T, Baum U, Harig F, et al. Visualization of a large ventricular aneurysm in a young man by 16-slice multi-detector row spiral computed tomography before successful surgical treatment. *Int J Cardiovasc Imaging.* 2006;22:537–41.
- Achenbach S, Ropers D, Daniel WG. Calcified left ventricular aneurysm. *N Engl J Med.* 2003;348:2469.
- Evangelou D, Letsas KP, Gavrielatos G, et al. Giant left-ventricular pseudoaneurysm following silent myocardial infarction. *Cardiology.* 2006;105:137–8.
- Makaryus AN, Manetta F, Goldner B, et al. Large left ventricular pseudoaneurysm presenting 25 years after penetrating chest trauma. *J Interv Cardiol.* 2005;18:193–200.
- Loures DRR, Carvalho RG, Lima Jr JD, et al. Tratamento cirúrgico dos aneurismas de ventrículo esquerdo e isquemia coronária. *Rev Bras Cir Cardiovasc.* 1997;12:122–31.
- Assunção FB, Oliveira DCL, Souza VF, et al. Cardiac magnetic resonance imaging and computed tomography in ischemic cardiomyopathy: an update. *Radiol Bras.* 2016;49:26–34.
- Rochitte CE. Cardiac MRI and CT: the eyes to visualize coronary arterial disease and their effect on the prognosis explained by the Schrödinger's cat paradox. *Radiol Bras.* 2016;49(1):vii–viii.
- Neves PO, Andrade J, Monção H. Coronary artery calcium score: current status. *Radiol Bras.* 2017;50:182–9.

**Kamila Seidel Albuquerque<sup>1</sup>, João Maurício Canavezi Indiani<sup>1</sup>, Marcelo Fontalvo Martin<sup>2</sup>, Beatriz Morais e Rodrigues Cunha<sup>2</sup>, Marcelo Souto Nacif<sup>2</sup>**

1. Unidade de Radiologia Clínica (URC), São José dos Campos, SP, Brazil. 2. Universidade Federal Fluminense (UFF), Niterói, RJ, Brazil. Mailing address: Dra. Kamila Seidel Albuquerque. Unidade de Radiologia Clínica. Rua Teopompo de Vasconcelos, 245, Vila Adyana. São José dos Campos, SP, Brazil, 12243-830. E-mail: kamilaseidel@hotmail.com.

<http://dx.doi.org/10.1590/0100-3984.2016.0199>



This is an open-access article distributed under the terms of the Creative Commons Attribution License.

## Bouveret syndrome and its imaging diagnosis

Dear Editor,

An 84-year-old female patient with hypertension reported pain in the upper abdomen accompanied by immediate postprandial nausea and vomiting, without gas or stool elimination for three days. The physical examination showed that she was afebrile, with a distended abdomen, pain upon deep palpation of the upper abdomen, and no signs of peritoneal irritation. A conventional X-ray of the abdomen (Figure 1A) showed air in a branched configuration in the hepatic projection and an air-fluid level in the gastric chamber. Ultrasound (Figure 1B) showed intrahepatic and extrahepatic bile ducts of normal size and the presence of pneumobilia, with no gallbladder identified. There was distension of the gastric chamber, the distal segment appearing to be adhered to the hepatic hilum, as well as a calculus in the pyloric antrum, suggesting the diagnostic hypothesis of gastric obstruction by a gallstone. For better diagnostic elucidation and evaluation of possible complications, we performed computed tomography of the abdomen (Figures 1C and 1D), which demonstrated a correlation with the ultrasound findings, confirming the imaging diagnosis of Bouveret syndrome.

Bouveret syndrome is a rare cause of gastric outlet obstruction due to large-scale impaction of a large gallstone in the duodenal bulb/pylorus after migration through a cholecystoduodenal/cholecystogastric fistula<sup>(1)</sup>. Gallstone ileus is a disease that mainly affects women, and the pathophysiology is often

explained by a previous episode of acute cholecystitis<sup>(2)</sup>. The incidence is highest in elderly individuals with comorbidities or biliary tract diseases. The following distribution of gallstone ileus sites has been described<sup>(1,3)</sup>: terminal ileum, 60%; proximal ileum, 24%; distal jejunum, 9%; colon and rectum, 2–4%; distal duodenum, 1–3%; and, less frequently, the proximal portion of the duodenum, where it causes immediate obstruction of emptying. Of all cases of gallstone ileus, 1–3% result from impacted stones in the pyloric or duodenal region, a condition known as Bouveret syndrome.

The diagnosis of Bouveret syndrome can be suspected on the basis of conventional X-ray findings, especially Rigler's triad (Rigler's sign), which is pathognomonic of gallstone ileus and appears in 40–50% of the cases in which conventional X-ray is employed. Rigler's triad is the combination of dilated loops with an air-fluid level, ectopic biliary lithiasis, and gas in the biliary tract<sup>(4)</sup>. Contrast-enhanced imaging of the upper digestive tract may be useful, with visualization of a filling defect, corresponding to the gallstone, and contrast enhancement of the orifice of the cholecystoduodenal/cholecystogastric fistula<sup>(3,5)</sup>. Ultrasound can show pneumobilia, gastric distension, and dilation of intestinal loops, as well as sometimes showing gallstones. Rigler's triad is most commonly seen on tomography scans, on which aerobic and gastric chamber dilatation are easily identified and the fistula can be diagnosed after administration of oral contrast, characterizing its leakage, or indirectly by the identification of contrast enhancement within the gallbladder<sup>(3)</sup>. Although prompt